

**Short Thesis for the Degree of Doctor of Philosophy  
(PhD)**

**Integration of Remotely Sensed Data and Field  
Studies for Lithological and Structural Mapping of  
Orogenic Gold Occurrences in the Barramiya–Mueilha  
Sector, Central Eastern Desert, Egypt**

By

Ali Shebl Ali Elshazly Rady

Supervisor: Dr. Árpád Csámer



**Doctoral School of Earth Sciences,  
University of Debrecen  
Debrecen, 2024**

## **Introduction**

Mineral resources and critical raw materials constitute the cornerstone of modern industries and underpin the economies of nations. While each country possesses its unique resource endowment, strategic investments in innovative exploration methods have the potential to yield groundbreaking discoveries in untapped areas, such as "greenfields," or optimize the utilization of existing mineralized terrains, known as "brownfields."

Recognizing the intrinsic relationship between geological exploration and economic advancement, this study embarks to evaluate and uncover prospective mineralized zones within the expansive canvas of the Egyptian Eastern Desert. Mineral potentiality mapping in such terrains has two main pillars. The first is accurate lithological mapping, where mineralized zones are mostly related to certain host rocks or lithological associations, so accurate lithological identification is a key to tracking and monitoring the mineralized hosts. The second pillar is structural analysis, considering that most of the gold deposits in these terrains are orogenic so a detailed structural analysis may uncover potential mineralized zones.

The first pillar revolves around the meticulous and precise delineation of lithological units. Mineralized

zones are intricately linked to specific host rocks and/ or lithological associations. Therefore, the accurate identification of lithological characteristics becomes a pivotal endeavor, facilitating the tracking and monitoring of mineralized hosts [1]–[3]. The second pillar centers on structural analysis. Significantly, the majority of gold deposits within these terrains are of orogenic origin, demanding a comprehensive structural analysis to unveil latent mineralized zones[4]–[8].

To achieve these goals, our research primarily dedicates itself to delivering precise lithological mapping. This pursuit seamlessly integrates cutting-edge techniques, incorporating a diverse range of datasets (multispectral, hyperspectral, and geophysical) and modern machine learning algorithms. The culmination of these investigations yields several insights regarding classifier performance and the optimal datasets for future lithological mapping within similar terrains. These results were even applied beyond the limits of the study area to test their efficiency and good findings were achieved and published in several journals.

Simultaneously, the structural analysis is meticulously explored through a dual-pronged approach. The first involves extracting lineaments utilizing a myriad of datasets, encompassing optical, radar, and digital elevation models (DEMs). The analysis extends to lineament density mapping, illuminating

highly dissected zones, which, when combined with hydrothermal alterations, offer a promising prospect for potential mineralization. A novel dimension of structural analysis is introduced through textural analysis, primarily grounded in correlation filters, revealing linear anomalies within the study area.

Drawing closer to our research objectives, a comprehensive hydrothermal alteration mapping is executed with precision, utilizing geophysical radiometric data and remote sensing techniques. Furthermore, structural complexity maps are crafted meticulously using geophysical magnetic data, augmenting our understanding of the structural landscape initially delineated via geophysical datasets[9].

The amalgamation of our research findings culminates in a spatial overlay analysis, effectively highlighting insights gleaned from preceding investigations. This multifaceted analysis enables us to pinpoint highly dissected regions and intensely altered zones, which are supposed to have mineralization potential. Fieldwork substantiates these deductions, reinforced by detailed petrographic examinations, and X-ray diffraction (XRD) analyses. Remarkably, during our field investigations of these high-potential zones, we have found current mining activities, closely mirroring our remote sensing and geophysical dataset findings.

## **Geological Setting of the study area**

The study area is situated within the Egyptian basement rocks, a constituent of the broader Arabian Nubian Shield (ANS). According to [10], [11], the ANS is recognized as the northern extension of the Mozambique belt, representing an example of accretionary orogens and suturing. Comprising primarily ophiolitic components and an island arc assemblage, the Egyptian basement rocks also feature significant intrusion of massive granitic formations [12]. Similar to the regional geology of the Egyptian basement rocks, the study area consists of imbricated layers of ophiolitic rocks intermingled with volcanic and sedimentary rocks from an island arc assemblage. The area exhibits granitoid and gabbroid intrusions [13], [14]. These intrusions have penetrated the pre-existing rocks, occasionally altering the primary structures [15]. The study area's southwestern region is overlaid by Phanerozoic Nubian sandstone, spanning from the Cambrian to the Upper Cretaceous period. The study area lies eastward of the Gabal Barramiya serpentinite and encompasses an extensive region stretching from Gabal El-Rukham in the north to Gabal Um Salatit and Dungash, to Gabal Mueilha in the south.

The main lithological groups in the study area include ophiolitic rocks, island arc metavolcanics, metagabbro-diorite rocks, granitic rocks (syn-orogenic and post-orogenic), post-granitic dykes, and Phanerozoic rocks. The ophiolitic rocks are mainly represented by

serpentinites and talc-carbonate rocks, with metagabbroic blocks within schistose volcanoclastic metasediments representing the melange matrix. Island arc assemblages are represented by metamorphosed (mainly greenschist facies) basic-intermediate metavolcanics (basaltic andesite to basalt), dacites, and pyroclastic tuffs/breccias [9], [13], [16]. Metagabbro-diorite rocks take on subcircular or irregular shapes intruding the ophiolitic, island arc metavolcanic, and metavolcanoclastic rocks.

On the other hand, these metagabbro-diorite complexes are intruded by granitic masses. The latter (syn- and post-orogenic) constitute extensive stretches extending north, south, and east beyond the studied area. The syn-orogenic granitoids are medium-grained, grey in color, and are quartz-diorite/granodiorite [16], exhibiting a sheared appearance and local schistosity. Late-orogenic granites are circular to subcircular and chiefly composed of alkali-feldspar granites such as Gabal Mueilha which has a prominent sharp contact with the surroundings.

These rocks exposed in the considered area are transected and traversed by a great number of dykes (ranging from mafic to felsic compositions). Phanerozoic cover is represented by Nubian Sandstone (Cambrian–Upper Cretaceous) exposures. They exhibit noticeable lithological variations and overlap unconformably with the Precambrian basement rocks.

## Applied Methods

### 1. Remote Sensing and Image Processing

Our remote sensing analysis employed several image processing techniques, including False Color Composite (FCC), Band Ratio, Relative Absorption Band Depth, Directed Principal Component Analysis (DPCA), and Constrained Energy Minimization Method (CEM). These methods were employed to enhance data quality and extract valuable spectral features for lithological identification and hydrothermal alteration delineation.

### 2. Machine Learning Algorithms (MLAs)

To process and extract relevant features from the data, we applied various methods, including Maximum Likelihood Classifier (MLC), Artificial Neural Networks (ANN), Support Vector Machine (SVM), Random Forest (RF), and Extreme Gradient Boosting (XGBoost)[17], [18]. These MLAs played a pivotal role in pattern recognition and classification lithological tasks by applying different mechanisms in the generalization process.

### 3. Structural Analysis

For structural analysis, we employed the LINE module for automatic lineament extraction. Key parameters, such as filter radius (RADI), edge gradient threshold (GTHR), curve length threshold (LTHR), line fitting threshold (FTHR), angular difference threshold

(ATHR), and linking distance threshold (DTHR), were meticulously adjusted to achieve accurate lineament extraction[15]. This analysis aimed to reveal significant structural elements within the study area.

Textural analysis was conducted using second-order statistical methods. Attributes including mean, variance, homogeneity, contrast, entropy, and correlation were computed to accentuate the principal structural characteristics within the study area.

#### 4. Airborne Geophysical Data Processing:

We applied several airborne geophysical data processing techniques, including the Center for Exploration Targeting (CET) porphyry analysis and the eTh/K ratio. These methods were instrumental in identifying areas with various types of hydrothermal alteration, such as potassic, phyllic, and propylitic alterations, as well as employing the 3D Euler deconvolution method.

#### 5. Field Investigations:

Extensive field investigations were conducted, involving camping in various regions of the study area. Over 100 field stations were established for sampling and studying the field relationships between exposed lithologies and associated hydrothermal alteration zones and structural elements.



## 6. Spatial Overlay Analysis

A spatial overlay analysis was performed within a Geographic Information System (GIS) environment. This analysis integrated all findings from remote sensing, structural analysis, geophysical data, and field investigations to highlight altered zones and generate a comprehensive understanding of the study area's geological features.

## 7. Petrographic, XRD, SEM-EDX, and Geochemical Analysis:

Our findings were rigorously validated through an array of laboratory-based analyses, including petrographic investigations, X-ray Diffraction (XRD) analysis, Scanning Electron Microscopy with Energy Dispersive X-ray Spectroscopy (SEM-EDX), and geochemical analysis. These analytical methods provided robust validation for our research outcomes.

## Thesis 1

**Stacked vector multi-sensor data is a more powerful input for machine learning algorithms and an effective approach in lithological mapping.**

Based on more than 110 classification analyses of common **multispectral** and radar remote sensing datasets, this study highlights the usefulness of SVM, MLC, and ANN in lithologic classification. SVM and

MLC consistently yield superior results compared to ANN. Furthermore, the study confirms that increasing data dimensionality (by increasing the number of utilized bands, denoted as N) is advantageous when sufficient training data is available, with a minimum requirement of  $30N$  training pixels for accurate classification.

## Thesis 2

**Introducing a novel approach (blending DEMs with multispectral datasets using SVM) for future lithological mapping enhancement.**

Each rock type exhibits distinct radiometric properties, magnetic characteristics, and varying responses to microwave and optical wavelengths. Likewise, it's expected that the same rock type generally shares common emplacement methods, textural features, and elevations for a certain study area (not over a global scale). Consequently, this study highlighted **the influence of rock unit elevation, obtained from DEMs**, on improving lithological mapping using optical datasets and SVM for classification. DEM significantly enhances classification performance compared to slope, aspect, Sentinel-1, and ALOS PALSAR data. S2, ASTER, and ALI are preferred over Landsat OLI for lithologic categorization. For more precise results, it is recommended to employ the combination of ALI, S2, ASTER, and DEM. The resultant lithological map (using

combined PALSAR DEM with multispectral data) introduced a well-defined distribution of all the rock units.

### Thesis 3

#### **Introducing SVM and XGB as powerful MLAs in PRISMA hyperspectral data analysis compared to RF and highlighting the potentiality of PRISMA for future Neoproterozoic rocks classifications**

For the first time over the study area and the entire ANS region, a new lithologic map was created using **PRISMA hyperspectral data** and various MLAs, including **RF, XGB, and SVM**. PRISMA hyperspectral data and their informative transformations, such as the first four principal components (PCs), prove effective for detailed lithological mapping in complex terrains with MLAs. While using PCA components (at least four PCs) aids in reducing data dimensionality for lithological discrimination, employing the full band set yields more accurate results. Among the MLAs, RF, XGB, and SVM are suitable choices with PRISMA data, **with SVM and XGB outperforming RF** in precise lithological allocation. Data gaps in certain bands may affect RF predictions compared to SVM and XGB. Following an exhaustive process involving visual interpretation, examination of existing geological maps, field surveys, and in-depth statistical analysis, this study highly advocates **the**

**utilization of XGB and SVM with PRISMA data for advancing lithological and mineralogical research.**

#### **Thesis 4**

**Introducing a novel lithological map of the study area with specifications of rock units (e.g. talc carbonates) rarely mapped before with such details.**

The doctoral thesis introduced **a new, objective lithologic map** of Um Salatit–Mueilha by discriminating a widely distributed stretch of Neoproterozoic ophiolitic mélange constituted mainly of allochthonous ophiolitic fragments embedded in a sheared matrix, as well as other different mappable units. The latter include metavolcanic, metagabbro-diorites, and granitic rocks. Our research resolved minute relationships among the closely related rocks e.g., serpentinites and talc carbonates within the same exposures as documented by our field observations.

#### **Thesis 5**

**DEMs (e.g., ALOS PALSAR) proved their leverage in lineament extraction (strongly recommended for future studies) and were able to effectively highlight the main structural setting of the study area as three main deformation phases (D1, D2, and D3).**

Our comprehensive structural analysis revealed that preferred lineament trends were classified into the

following main categories: (1) NNE-SSW to NNW-SSE, (2) ENE-WSW to WNW-ESE, (3) NE-SW, and (4) NW-SE. These findings align seamlessly with previous geological studies and our field investigations, reaffirming their accuracy and the efficiency of the adopted method. This study (based on previous research) also organized deformation phases and related structures into three main phases: **D1, D2, and D3**. D1 corresponds to NNW-SSE shortening, leading to NE-SW trending structures, while D2 results in NNE-SSW shortening and NW-SE trends. Notably, ENE-WSW to WNW-ESE trends arise from the combined influence of D1 and D2, while NNE-SSW to NNW-SSE trends are attributed to the D3 phase, known as E-W Oblique Convergence.

## **Thesis 6**

**Novel insights into structural features could be gained through textural analysis. Textural analysis greatly helps in resolving complex structural patterns such as lineaments, folds, and foliations.**

The research presents a simplified approach aimed at overcoming the dimensionality challenges often associated with remote sensing data. We achieved this by employing different kernel sizes (3×3, 7×7, 11×11) on individual Sentinel 2 bands (2.5m and 10m) to extract a

range of textural attributes, including mean, variance, homogeneity, contrast, entropy, and correlation. By combining these **textural patterns**, we were able to extract diverse information, which greatly aids in geological interpretations for further investigations. For highly accurate structural mapping, the use of **correlation data** is recommended, as it captures linear dependencies and enables the robust identification of various structural features including **foliations, folding, and fracturing**. The most effective combination for superior structural results involves using correlation, mean, and variance in the RGB channels, respectively.

## Thesis 7

**Utilizing airborne geophysical and multi-sensor remote sensing data enables improved delineation of hydrothermal alterations. This integrated approach reveals the prevalence of OH-bearing minerals and iron oxides within the study area.**

Utilizing the recommended integrated Geophysical data, Sentinel 2, and ASTER images, **our study identified alteration zones** that align with magnetic and radiometrically altered regions characterized by **high magnetic and high K/eTh ratio anomalies**, indicative of metalliferous minerals. These zones are **closely associated with shear zones** in the study area. **Depth estimation** analysis revealed that

while most anomalies originate from shallow depths (0–600 m), some deeper anomalies extend down to 1500 m. This investigation unveils the hydrothermal alteration patterns, primarily featuring **OH-bearing minerals and iron oxides**. It provides insights into the structural framework of the surveyed region through the integration of various data sources and scales, including satellite remote sensing imagery, airborne geophysical data, fieldwork, and petrographic examinations. These findings can significantly improve the identification of genuine alteration zones for future feasibility studies and exploitation endeavors.

## Thesis 8

**Multiscale lab investigations (thin sections, XRD, and SEM) are a powerful approach to mineral exploration theme. Detailed petrographic investigations, XRD, and SEM analysis revealed the prevalence of carbonatization, ferrugination, argillitization, propylitization, serpentization, and phyllitization within the study area. Gold grains were mainly detected under SEM within quartz veins and altered zones.**

Petrographic investigations, XRD analysis, and SEM-EDX, were performed to **better characterize the lithological units and hydrothermal alteration zones** within the study area. Investigating **thin sections** of

representative rock samples from the various rock exposures in the Um Salatit-Mueilha area highlighted the dominance of the ophiolitic group association. The latter is represented by serpentinites, talc carbonates, metagabbros, and ophiolitic mélange. Additionally, island arc metavolcanic (mainly metaandesites or basaltic metaandesites), metagabbro-diorite complex, older, and younger granites, and post-granitic dykes are represented within the study area. **XRD analysis** revealed an intensive and wide range of alterations represented by carbonatization, ferrugination, argillitization, propylitization, serpentinization, and phyllitization.

**SEM images** uncovered a prevalence of gold mineralization in numerous samples, alongside a diverse spectrum of other ores, such as iron oxides (magnetite, hematite), scheelite ( $\text{CaWO}_4$ ), marcasite, pyrrhotite, pyrite, molybdenite, W-bearing rutile, and Baddeleyite ( $\text{ZrO}_2$ ), primarily within quartz veins. Gold was discerned in several veins, manifesting in different forms, including electrum (a naturally occurring gold-silver alloy) or pure gold grains. Additionally, a void-filling late-stage calcite was identified surrounding quartz and gold grains.



## Thesis 9

**Whole-rock geochemistry revealed the classification and characteristics of the studied rock units, and most importantly, confirmed the presence of gold in all samples analyzed by SEM-EDX.**

Geochemical classifications of the metavolcanic varieties categorize them primarily as **andesitic and andesite-basalt types**, with minor occurrences of dacitic and rhyolitic rocks. These metavolcanic formations constitute a collection of mildly altered calc-alkaline volcanic rocks, primarily composed of andesite-dacite compositions. In contrast, the plutonic rock samples are found in regions corresponding to **gabbros, diorites, alkali-granite, and granodiorite-tonalite** compositions. These findings are in excellent agreement with other multiscale analyses, including remote sensing, field observations, petrography, and XRD analysis. Further alkalinity analysis reveals that the metavolcanic rocks fall under the sub-alkaline umbrella, predominantly aligning with andesite to basaltic classifications, while the plutonic specimens represent another sub-alkaline rock series. It should be emphasized that there was a considered agreement between all the integrated tools in the current research. For instance, altered zones detected using remote sensing data were verified in the field through handspecimens and thin sections, as well as through XRD analysis. Additionally, samples bearing

gold identified during SEM analysis exhibited higher gold content in our geochemical analysis.

## References

- [1] H. M. El-Desoky *et al.*, "Multiscale mineralogical investigations for mineral potentiality mapping of Ras El-Kharit-Wadi Khashir district, Southern Eastern Desert, Egypt," *Egypt. J. Remote Sens. Sp. Sci.*, vol. 25, no. 4, pp. 941–960, Dec. 2022, doi: 10.1016/J.EJRS.2022.09.001.
- [2] R. Amer, T. Kusky, and A. Ghulam, "Lithological mapping in the Central Eastern Desert of Egypt using ASTER data," *J. African Earth Sci.*, vol. 56, no. 2, pp. 75–82, 2010, doi: <https://doi.org/10.1016/j.jafrearsci.2009.06.004>.
- [3] M. Z. Khedr *et al.*, "Remote sensing techniques and geochemical constraints on the formation of the Wadi El-Hima mineralized granites, Egypt: new insights into the genesis and accumulation of garnets," *Int. J. Earth Sci.*, vol. 111, no. 7, pp. 2409–2443, Aug. 2022, doi: 10.1007/S00531-022-02237-7/TABLES/1.
- [4] M. Badawi, M. Abdelatif, A. Shebl, F. Makroum, A. Shalaby, and N. Nemeth, "Mapping Structurally Controlled Alterations Sparked by Hydrothermal Activity in the Fatira-Abu Zawal

Area, Eastern Desert, Egypt," *Acta Geol. Sin. - English Ed.*, Nov. 2022, doi: 10.1111/1755-6724.15019.

- [5] B. Zoheir, "Transpressional zones in ophiolitic mélange terranes: Potential exploration targets for gold in the South Eastern Desert, Egypt," *J. Geochemical Explor.*, vol. 111, no. 1, pp. 23–38, 2011, doi: <https://doi.org/10.1016/j.gexplo.2011.07.003>.
- [6] M. C. Reinhardt and I. Davison, "Structural and lithologic controls on gold deposition in the shear zone-hosted Fazenda Brasileiro Mine, Bahia State, Northeast Brazil," *Econ. Geol.*, vol. 85, no. 5, pp. 952–967, Aug. 1990, doi: 10.2113/GSECONGEO.85.5.952.
- [7] M. A. Abd El-Wahed, "Oppositely dipping thrusts and transpressional imbricate zone in the Central Eastern Desert of Egypt," *J. African Earth Sci.*, vol. 100, pp. 42–59, Dec. 2014, doi: 10.1016/J.JAFREARSCI.2014.06.010.
- [8] R. J. Goldfarb, T. Baker, B. Dubé, D. I. Groves, C. J. R. Hart, and P. Gosselin, "Distribution, Character, and Genesis of Gold Deposits in Metamorphic Terran," *One Hundredth Anniv. Vol.*, Oct. 2005, doi: 10.5382/AV100.14.
- [9] A. Shebl, M. Abdellatif, M. Badawi, M. Dawoud, A. S. Fahil, and Á. Csámer, "Towards better

delineation of hydrothermal alterations via multi-sensor remote sensing and airborne geophysical data," *Sci. Rep.*, vol. 13, no. 1, p. 7406, 2023.

- [10] R. J. Stern, "Arc-assembly and continental collision in the Neoproterozoic African orogen: implications for the consolidation of Gondwanaland," *Annu. Rev. Earth Planet. Sci.*, vol. 22, pp. 319–351, 1994.
- [11] M. G. Abdelsalam and R. J. Stern, "Sutures and shear zones in the Arabian-Nubian Shield," *J. African Earth Sci.*, vol. 23, no. 3, pp. 289–310, 1996.
- [12] R. . Shackleton, "Contrasting structural relationships of Proterozoic ophiolites in Northeast and Eastern Africa," *Contrasting Struct. relationships Proterozoic ophiolites Northeast East. Africa*, 1988.
- [13] A. Shebl, T. Kusky, and Á. Csámer, "Advanced land imager superiority in lithological classification utilizing machine learning algorithms," *Arab. J. Geosci.* 2022 159, vol. 15, no. 9, pp. 1–13, May 2022, doi: 10.1007/S12517-022-09948-W.
- [14] B. Zoheir, M. A. El-Wahed, A. B. Pour, and A. Abdelnasser, "Orogenic gold in transpression and transtension zones: Field and remote sensing studies of the barramiya–mueilha sector, Egypt," *Remote Sens.*, vol. 11, no. 18, p. 2122, 2019.

- [15] A. Shebl and Á. Csámer, "Reappraisal of DEMs, Radar and optical datasets in lineaments extraction with emphasis on the spatial context," *Remote Sens. Appl. Soc. Environ.*, vol. 24, p. 100617, Nov. 2021, doi: 10.1016/J.RSASE.2021.100617.
- [16] B. Zoheir and P. Weihed, "Greenstone-hosted lode-gold mineralization at Dungash mine, Eastern Desert, Egypt," *J. African Earth Sci.*, vol. 99, pp. 165–187, 2014.
- [17] A. Shebl, D. Abriha, A. S. Fahil, H. A. El-Dokouny, A. A. Elrasheed, and Á. Csámer, "PRISMA hyperspectral data for lithological mapping in the Egyptian Eastern Desert: Evaluating the Support Vector Machine, Random Forest, and XG Boost Machine Learning Algorithms," *Ore Geol. Rev.*, p. 105652, 2023.
- [18] A. Shebl and Á. Csámer, "Stacked vector multi-source lithologic classification utilizing Machine Learning Algorithms: Data potentiality and dimensionality monitoring," *Remote Sens. Appl. Soc. Environ.*, p. 100643, Oct. 2021, doi: 10.1016/J.RSASE.2021.100643.



Registry number: DEENK/317/2024.PL  
Subject: PhD Publication List

Candidate: Ali Shebl  
Doctoral School: Doctoral School of Earth Sciences  
MTMT ID: 10080139

### List of publications related to the dissertation

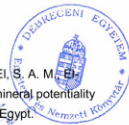
#### Foreign language scientific articles in international journals (16)

1. **Shebl, A.**, Badawi, M., Dawoud, M., Abd El, W. M., El-Dokouny, H. A., Csámer, Á.: Novel comprehensions of lithological and structural features gleaned via Sentinel 2 texture analysis. *Ore Geol. Rev.* 168, 1-26, 2024. ISSN: 0169-1368.  
DOI: <http://dx.doi.org/10.1016/j.oregeorev.2024.106068>  
IF: 3.3 (2022)
2. Dawoud, M., Khalaf, I. M., El-Dokouny, H. A., **Shebl, A.**, El, D. H. A., El, L. M. A.: Applications of remote sensing in lithological mapping of east Gabal Atud area, central eastern desert, Egypt. *Geo-Eco-Marina.* 29, 125-146, 2023. ISSN: 1224-6808.  
DOI: <http://dx.doi.org/10.5281/zenodo.10254865>
3. El-Desoky, H. M., **Shebl, A.**, El-Awny, H., El-Rahmany, M. M., Soliman, O.: Detecting Oxides Mineralization Utilizing Remote Sensing and Comprehensive Mineralogical Analysis: A Case Study Around Mikbi-Zayatit District, South Eastern Desert, Egypt. *Iraqi Geological Journal.* 56 (1E), 97-130, 2023. ISSN: 2414-6064.  
DOI: <http://dx.doi.org/10.46717/igj.56.1E.8ms-2023-5-18>
4. **Shebl, A.**, El-Desoky, H. M., Abdel-Rahman, A. M., Fahmy, W., El-Awny, H., El, S. A. M., El-Rahmany, M. M., Csámer, Á.: Impact of DEMs for Improvement Sentinel 2 Lithological Mapping Utilizing Support Vector Machine: A Case Study of Mineralized Fe-Ti-Rich Gabbroic Rocks from the South Eastern Desert of Egypt. *Minerals.* 13 (6), 1-36, 2023. EISSN: 2075-163X.  
DOI: <http://dx.doi.org/10.3390/min13060826>  
IF: 2.5 (2022)
5. Badawi, M., Abdelatif, M., **Shebl, A.**, Makroum, F., Shalaby, T., Németh, N.: Mapping Structurally Controlled Alterations Sparked by Hydrothermal Activity in the Fatira-Abu Zawal Area, Eastern Desert, Egypt. *Acta Geol. Sin.-Engl. Ed.* 97 (2), 662-680, 2023. ISSN: 1000-9515.  
DOI: <http://dx.doi.org/10.1111/1755-6724.15019>  
IF: 3.3 (2022)





6. **Shebl, A.**, Hamdy, M.: Multiscale (microscopic to remote sensing) preliminary exploration of auriferous-uraniferous marbles: A case study from the Egyptian Nubian Shield.  
*Sci. Rep.* 13 (1), 1-24, 2023. EISSN: 2045-2322.  
DOI: <http://dx.doi.org/10.1038/s41598-023-36388-7>  
IF: 4.6 (2022)
7. **Shebl, A.**, Aabriha, D., Fahil, A. S., El-Dokouny, H. A., Abdelmajeed, A. E. A., Csámer, Á.: PRISMA hyperspectral data for lithological mapping in the Egyptian Eastern Desert: Evaluating the support vector machine, random forest, and XG boost machine learning algorithms.  
*Ore Geol. Rev.* 161, 1-16, 2023. ISSN: 0169-1368.  
DOI: <http://dx.doi.org/10.1016/j.oregeorev.2023.105652>  
IF: 3.3 (2022)
8. Abdel-Rahman, A. M., El-Desoky, H. M., **Shebl, A.**, El-Awmy, H., Amer, Y. Z., Csámer, Á.: The geochemistry, origin, and hydrothermal alteration mapping associated with the gold-bearing quartz veins at Hamash district, South Eastern Desert, Egypt.  
*Sci. Rep.* 13 (1), 1-27, 2023. EISSN: 2045-2322.  
DOI: <http://dx.doi.org/10.1038/s41598-023-42313-9>  
IF: 4.6 (2022)
9. **Shebl, A.**, Abdellatif, M., Badawi, M., Dawoud, M., Fahil, A. S., Csámer, Á.: Towards better delineation of hydrothermal alterations via multi-sensor remote sensing and airborne geophysical data.  
*Sci. Rep.* 13 (1), 1-27, 2023. EISSN: 2045-2322.  
DOI: <http://dx.doi.org/10.1038/s41598-023-34531-y>  
IF: 4.6 (2022)
10. **Shebl, A.**, Kusky, T., Csámer, Á.: Advanced land imager superiority in lithological classification utilizing machine learning algorithms.  
*Arab. J. Geosci.* 15 (9), 1-13, 2022. ISSN: 1866-7511.  
DOI: <http://dx.doi.org/10.1007/s12517-022-09948-w>
11. Abdelkader, M. A., Watanabe, Y., **Shebl, A.**, El-Dokouny, H. A., Dawoud, M., Csámer, Á.: Effective delineation of rare metal-bearing granites from remote sensing data using machine learning methods: A case study from the Umm Naggat Area, Central Eastern Desert, Egypt.  
*Ore Geol. Rev.* 150, 1-26, 2022. ISSN: 0169-1368.  
DOI: <http://dx.doi.org/10.1016/j.oregeorev.2022.105184>  
IF: 3.3
12. El-Desoky, H. M., **Shebl, A.**, Abdel-Rahman, A. M., Fahmy, W., El-Awmy, H., El-Sayid, M. M., El-Rahmany, M. M., Csámer, Á.: Multiscale mineralogical investigations for mineral potentiality mapping of Ras El-Kharit-Wadi Khashir district, Southern Eastern Desert, Egypt.  
*Egypt. J. Remote Sensing Space Sci.* 25 (4), 941-960, 2022. ISSN: 1110-9823.  
DOI: <http://dx.doi.org/10.1016/j.ejrs.2022.09.001>





13. **Shebl, A., Abdellatif, M., Hissen, M., Ibrahim Abdelaziz, M., Csámer, Á.:** Lithological mapping enhancement by integrating Sentinel 2 and gamma-ray data utilizing support vector machine: A case study from Egypt.  
*Int. J. Appl. Earth Obs. Geoinf.* 105, 1-16, 2021. ISSN: 1569-8432.  
DOI: <http://dx.doi.org/10.1016/j.jag.2021.102619>  
IF: 7.672
14. **Shebl, A., Abdellatif, M., Elkhateeb, S. O., Csámer, Á.:** Multisource Data Analysis for Gold Potentiality Mapping of Atalla Area and Its Environs, Central Eastern Desert, Egypt.  
*Minerals.* 11 (6), 1-19, 2021. EISSN: 2075-163X.  
DOI: <http://dx.doi.org/10.3390/min11060641>  
IF: 2.818
15. **Shebl, A., Csámer, Á.:** Reappraisal of DEMs, Radar and optical datasets in lineaments extraction with emphasis on the spatial context.  
*Remote Sens. Appl.* 24, 1-12, 2021. ISSN: 2352-9385.  
DOI: <http://dx.doi.org/10.1016/j.rsase.2021.100617>
16. **Shebl, A., Csámer, Á.:** Stacked vector multi-source lithologic classification utilizing Machine Learning Algorithms: Data potentiality and dimensionality monitoring.  
*Remote Sens. Appl.* 24, 1-9, 2021. ISSN: 2352-9385.  
DOI: <http://dx.doi.org/10.1016/j.rsase.2021.100643>

Foreign language conference proceedings (1)

17. **Shebl, A., Csámer, Á.:** Lithological, structural and hydrothermal alteration mapping utilizing remote sensing datasets: a case study around Um Salim area, Egypt.  
*IOP Conf. Ser.: Earth Environ. Sci.* 942 (1), 1-8, 2021. ISSN: 1755-1307.  
DOI: <http://dx.doi.org/10.1088/1755-1315/942/1/012032>







13. **Shebl, A., Abdellatif, M., Hissen, M., Ibrahim Abdelaziz, M., Csámer, Á.:** Lithological mapping enhancement by integrating Sentinel 2 and gamma-ray data utilizing support vector machine: A case study from Egypt.  
*Int. J. Appl. Earth Obs. Geoinf.* 105, 1-16, 2021. ISSN: 1569-8432.  
DOI: <http://dx.doi.org/10.1016/j.jag.2021.102619>  
IF: 7.672
14. **Shebl, A., Abdellatif, M., Elkhateeb, S. O., Csámer, Á.:** Multisource Data Analysis for Gold Potentiality Mapping of Atalla Area and Its Environs, Central Eastern Desert, Egypt.  
*Minerals.* 11 (6), 1-19, 2021. EISSN: 2075-163X.  
DOI: <http://dx.doi.org/10.3390/min11060641>  
IF: 2.818
15. **Shebl, A., Csámer, Á.:** Reappraisal of DEMs, Radar and optical datasets in lineaments extraction with emphasis on the spatial context.  
*Remote Sens. Appl.* 24, 1-12, 2021. ISSN: 2352-9385.  
DOI: <http://dx.doi.org/10.1016/j.rsase.2021.100617>
16. **Shebl, A., Csámer, Á.:** Stacked vector multi-source lithologic classification utilizing Machine Learning Algorithms: Data potentiality and dimensionality monitoring.  
*Remote Sens. Appl.* 24, 1-9, 2021. ISSN: 2352-9385.  
DOI: <http://dx.doi.org/10.1016/j.rsase.2021.100643>

Foreign language conference proceedings (1)

17. **Shebl, A., Csámer, Á.:** Lithological, structural and hydrothermal alteration mapping utilizing remote sensing datasets: a case study around Um Salim area, Egypt.  
*IOP Conf. Ser.: Earth Environ. Sci.* 942 (1), 1-8, 2021. ISSN: 1755-1307.  
DOI: <http://dx.doi.org/10.1088/1755-1315/942/1/012032>





List of other publications

Foreign language international book chapters (1)

18. **Shebl, A.**, Mohamed, A. A., Csámer, Á.: Vertical accuracy assessment of DEMs around Jabal al-Shayeb area, Egypt.  
In: The proceedings of the 3rd Intercontinental Geoinformation Days / Prof. Dr. Murat YAKAR, Mersin University, Mersin, 42-45, 2023. ISBN: 9786254430374

Foreign language scientific articles in international journals (3)

19. Ghoneim, E., Healey, C., Hemida, M., **Shebl, A.**, Fahil, A. S.: Integration of Geophysical and Geospatial Techniques to Evaluate Geothermal Energy at Siwa Oasis, Western Desert, Egypt.  
*Remote Sens.* 15 (21), 1-19, 2023. EISSN: 2072-4292.  
DOI: <http://dx.doi.org/10.3390/rs15215094>  
IF: 5 (2022)
20. **Shebl, A.**, Abdelaziz, M. I., Ghazala, H., Araffa, S. A. S., Abdellatif, M., Csámer, Á.: Multi-criteria ground water potentiality mapping utilizing remote sensing and geophysical data: A case study within Sinai Peninsula, Egypt.  
*Egypt. J. Remote Sensing Space Sci.* 25 (3), 765-778, 2022. ISSN: 1110-9823.  
DOI: <http://dx.doi.org/10.1016/j.ejrs.2022.07.002>
21. Abd El, W. M., Kamh, S., Ashmawy, M., **Shebl, A.**: Transpressive Structures in the Ghadir Shear Belt, Eastern Desert, Egypt: Evidence for Partitioning of Oblique Convergence in the Arabian-Nubian Shield during Gondwana Agglutination.  
*Acta Geol. Sin.-Engl. Ed.* 93 (6), 1614-1646, 2019. ISSN: 1000-9515.  
DOI: <http://dx.doi.org/10.1111/1755-6724.13882>  
IF: 1.973

**Total IF of journals (all publications): 46,963**

**Total IF of journals (publications related to the dissertation): 39,99**

The Candidate's publication data submitted to the IDEa Tudóster have been validated by DEENK on the basis of the Journal Citation Report (Impact Factor) database.



29 May, 2024